Hall Noise and Transverse Freezing in Driven Vortex Lattices

Alejandro B. Kolton and Daniel Domínguez
Centro Atómico Bariloche, 8400 S. C. de Bariloche, Rio Negro, Argentina

Niels Grønbech-Jensen
Theoretical Division, Los Alamos National Laboratory, Los Alamos, New Mexico 87545
(Received 11 June 1999)

We study driven vortex lattices in superconducting thin films. Above the critical force F_c we find two dynamical phase transitions at F_p and F_t, which could be observed in simultaneous noise measurements of the longitudinal and Hall voltage. At F_p there is a transition from plastic flow to smectic flow, where the voltage noise is isotropic (Hall noise = longitudinal noise) and there is a peak in the differential resistance. At F_t there is a sharp transition to a frozen transverse solid, where the Hall noise falls abruptly and vortex motion is localized in the transverse direction.

PACS numbers: 74.60.Ge, 05.70.Fh, 74.40.+k

The study of the collective motion of vortex lattices in superconductors has brought new concepts into the nonequilibrium statistical physics of driven disordered media [1–18]. The prediction [1] of a *dynamical phase transition* upon increasing drive, from a fluidlike plastic flow regime [2–4] to a coherently moving solid [1], has motivated an outburst of recent theoretical [5–7], experimental [8–11], and simulation [12–18] work. The relevant physics of the high velocity driven phase is controlled by the transverse displacements (in the direction perpendicular to the driving force) [5], leading to a new class of driven systems characterized by *anisotropic spatial structures* with transverse periodicity [5–7]. Recently, these moving anisotropic vortex structures have been observed experimentally by Pardo *et al.* [11], and their different features have been studied in 2D [12–16] and 3D [17,18] simulations. It was proposed that temporal correlations may be a useful characterization of nonequilibrium driven systems [19]. In fact, we will show here that a good insight into the moving phases can be obtained from studying the *anisotropic temporal fluctuations*. We find two dynamical phase transitions which could be observed experimentally by measuring voltage noise [20,21], both in the longitudinal and transversal directions.

The equation of motion of a vortex in position $\mathbf{r}_i$ is

$$\eta \frac{d\mathbf{r}_i}{dt} = -\sum_{j\neq i} \nabla_i U_v(r_{ij}) - \sum_p \nabla_i U_p(r_{ip}) + \mathbf{F}, \qquad (1)$$

where $r_{ij} = |\mathbf{r}_i - \mathbf{r}_j|$ is the distance between vortices i, j, $r_{ip} = |\mathbf{r}_i - \mathbf{r}_p|$ is the distance between the vortex i and a pinning site at $\mathbf{r}_p$, $\eta = \frac{\Phi_0 H_{c2} d}{c^2 \rho_n}$ is the Bardeen-Stephen friction, and $\mathbf{F} = \frac{d\Phi_0}{c}\mathbf{J} \times \mathbf{z}$ is the driving force due to an applied current $\mathbf{J}$. A two-dimensional superconductor is realized in thin films of thickness d, where $d \ll \lambda$, which have an effective penetration depth $\Lambda = 2\lambda^2/d$. Since Λ is of the order of the sample size ($\Lambda \approx 200\ \mu$m in [9]), the vortex-vortex interaction is logarithmic: $U_v(r) = -A_v \ln(r/\Lambda)$, with $A_v = \Phi_0^2/8\pi\Lambda$ [3,13]. The vortices interact with a random uniform distribution of attractive pinning centers with $U_p(r) = -A_p e^{-(r/\xi)^2}$ with ξ being the coherence length. We normalize length scales by ξ, energy scales by A_v, and time is normalized by $\tau = \eta\xi^2/A_v$. We consider N_v vortices and N_p pinning centers in a rectangular box of size $L_x \times L_y$, and the normalized vortex density is $n_v = N_v\xi^2/L_xL_y = B\xi^2/\Phi_0$. Moving vortices induce a total electric field $\mathbf{E} = \frac{B}{c}\mathbf{v} \times \mathbf{z}$, with $\mathbf{v} = \frac{1}{N_v}\sum_i \mathbf{v}_i$.

We study the dynamical regimes in the velocity-force (voltage-current) characteristics at $T = 0$, solving Eq. (1) for increasing values of $\mathbf{F} = F\mathbf{y}$. We consider a constant vortex density $n_v = 0.12$ in a box with $L_x/L_y = \sqrt{3}/2$, and $N_v = 64$, 144, 196, 256, 400, and 784 (we show results for $N_v = 400$). We take a pinning strength of $A_p/A_v = 0.2$ with a density of pinning centers $n_p = 0.24$. We use periodic boundary conditions, and the periodic long-range logarithmic interaction is evaluated with an exact and fast converging sum [22]. The equations are integrated with a time step of $\Delta t = 0.01\tau$, and averages are evaluated in 32 768 integration steps after 2000 iterations for equilibration (when the total energy reaches a stationary value). Each simulation is started at $F = 0$ with an ordered triangular lattice and by slowly increasing the force in steps of $\Delta F = 0.05$ up to values as high as $F = 8$.

We start by looking at the vortex trajectories and their translational order in the steady state phases as was done in Refs. [12–18]. In Figs. 1(a)–1(c) we show the vortex trajectories $\{\mathbf{r}_i(t)\}$ for typical values of F by plotting all the positions of the vortices for all the time iteration steps. We also study the time-averaged structure factor $S(\mathbf{k}) = \langle|\frac{1}{N_v}\sum_i \exp[i\mathbf{k}\cdot\mathbf{r}_i(t)]|^2\rangle$, which is shown in Figs. 1(d)–1(f). In Fig. 2(a) we plot the average vortex velocity $V = \langle V_y(t)\rangle = \langle\frac{1}{N_v}\sum_i \frac{dy_i}{dt}\rangle$, in the direction of the force as a function of F and its corresponding derivative dV/dF. ($V = E/\rho_f J_0$ with ρ_f the flux flow resistivity and

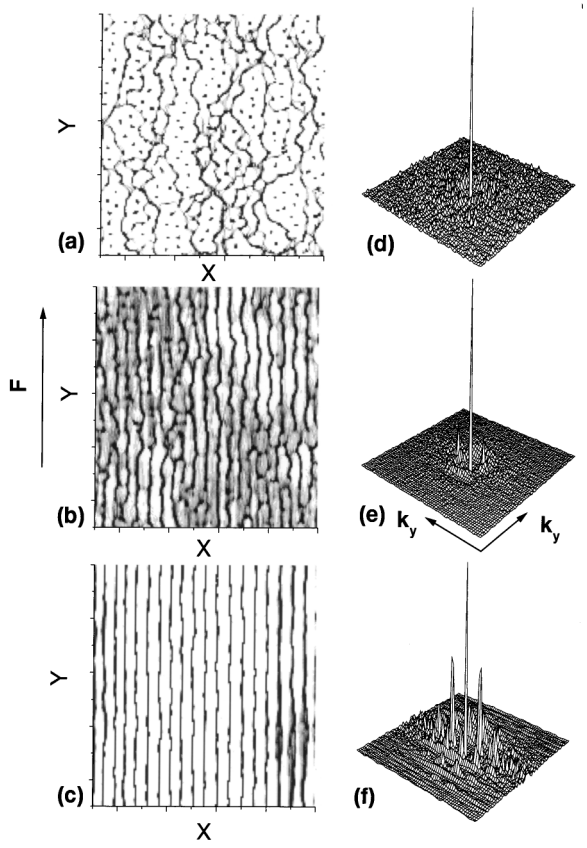

FIG. 1. Vortex trajectories: (a) $F = 0.5$, (b) $F = 2.5$, and (c) $F = 7$. Surface intensity plot of the averaged structure factor $S(\mathbf{k})$: (d) $F = 0.5$, (e) $F = 2.5$, and (f) $F = 7$.

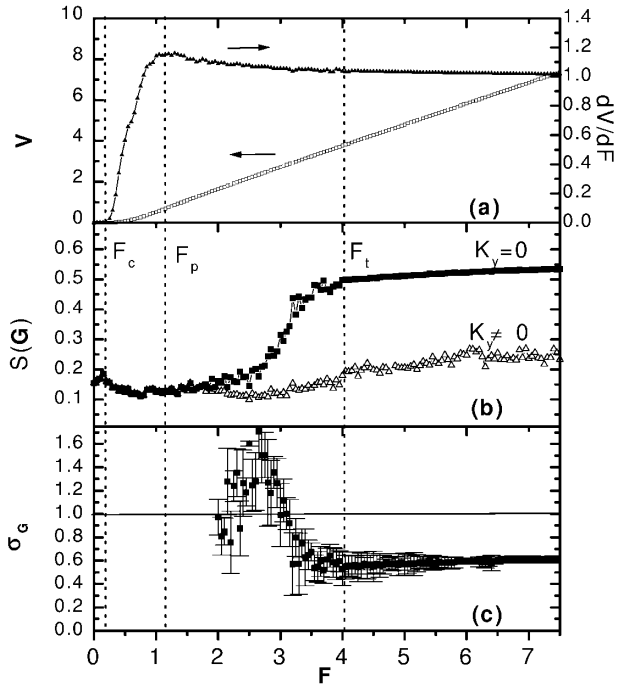

FIG. 2. (a) Velocity-force curve (voltage-current characteristics), left scale, white points. dV/dF curve (differential resistance), right scale, black points. (b) Intensity of the Bragg peaks. For smectic ordering $S(G_1)$, $K_y = 0$: black points. For longitudinal ordering $S(G_{2,3})$, $K_y \neq 0$: white points. (c) Finite size exponent σ_G $[S(G_1) \sim N_v^{-\sigma_G}]$.

$J_0 = cA_v/d\xi\Phi_0$; therefore, dV/dF is proportional to the differential resistivity $dV/dF = \rho_f^{-1} dE/dJ$). Below a critical force $F_c \approx 0.25$ all the vortices are pinned and there is no motion, $V = 0$. Above F_c, we distinguish among three different dynamical regimes.

(i) Plastic flow: $F_c < F < F_p$.—At F_c, vortices start to move in a few filamentary channels, as was also seen in [3]. A typical situation is shown in Fig. 1(a), where a fraction of the vortices are moving in an intricate network of channels. As the force is increased a higher fraction of vortices is moving. In this regime, vortices can move in the transverse direction (perpendicular to **F**) through the tortuous structure of channels [4]. We see in Fig. 1(d) that $S(\mathbf{k})$ only has the central peak showing the absence of ordering in this plastic flow regime [2–4].

(ii) Smectic flow: $F_p < F < F_t$.—We observe a peak in the differential resistance at a characteristic force $F_p \approx 1.3$. At $F = F_p$ we see that *all* the vortices are moving in a seemingly isotropic channel network with maximum interconnectivity. In other simulations the peak in the differential resistance was found to coincide with a maximum in the number of defects [15] and with the onset of orientational order [13]. Also, the value of F_p was taken in the experiment of Hellerqvist *et al.* [9] as an indication of a dynamical phase transition. In fact, we find that above F_p a new dynamic regime sets in. In this case, as we show in Fig. 1(b), all the vortices are moving in trajectories that are mostly parallel to the force, forming "elastic channels." Two small Bragg peaks appear in the structure factor along the $K_y = 0$ axis, as seen in Fig. 1(e), which correspond to $\mathbf{G}_1 = (\pm 2\pi/a_0, 0)$. This is consistent with the onset of "smectic" ordering [6,12] in the transverse direction with elastic channels separated by a distance $\sim a_0 = n_v^{-1/2}$. In this regime the transverse motion consists of vortex jumps from one channel to another, resembling "thermally" activated transitions induced by local chaos. The rate of these transitions decreases with increasing force, and they correspond to the permeation modes discussed in [6]. In Fig. 2(b) we plot the magnitude of the Bragg peaks at G_1, $S_s = S(G_1)$, corresponding to smectic ordering ($K_y = 0$), and the other neighboring peaks at $\mathbf{G}_2 = \pm 2\pi/a_0(1/2, \sqrt{3}/2)$ and $\mathbf{G}_3 = \pm 2\pi/a_0(-1/2, \sqrt{3}/2)$, $S_l = [S(G_2) + S(G_3)]/2)$, corresponding to longitudinal ordering ($K_y \neq 0$). We see that above F_p the intensity of the smectic peak S_s starts to grow and $S_s \gg S_l$, while below F_p the spatial structure is isotropic, $S_s = S_l \ll 1$. The Bragg peak heights depend on system size as $S(G) \sim N_v^{-\sigma_G}$, where $\sigma_G = 0$ means long-range order, $0 < \sigma_G < 1$ means quasi-long-range order (QLRO), and $\sigma_G = 1$ means short-range order. In Fig. 2(c) we show the corresponding results for the smectic peak $S_s = S(G_1)$

for sizes $N_v = 256$, 400, and 784. We see that $\sigma_G \gtrsim 1$ in this regime: there is only short-range smectic order, thus this phase corresponds to a liquid. In this sense the transition at F_p is a dynamic transition in the flow, as found in [16] for strong disorder ($n_p = 1$). When approaching F_t (see below) we see a precursor of QLRO ($\sigma_g < 1$) but with strong fluctuations.

(iii) Frozen transverse solid: $F > F_t$.—At a new characteristic force F_t, the jumps between channels suddenly stop and vortex motion becomes frozen in the direction perpendicular to **F**. An example of $F > F_t$ is shown in Fig. 1(c) where we see well-defined elastic channels parallel to **F**. The corresponding structure factor is in Fig. 1(e), where new peaks appear in $S(\mathbf{k})$ in directions with $K_y \neq 0$, such as G_2, G_3, showing that there is some longitudinal ordering between the channels. These extra peaks are smaller than the smectic peaks, and $S(\mathbf{k})$ is very anisotropic. We note in Fig. 2(a) that F_t is the point where the noisy behavior in dV/dF ceases. A similar criterion was used by Bhattacharya and Higgins to define their dynamical phase diagram [8]. In Fig. 2(b) we see that in F_t there is an increase in the longitudinal ordering S_l, and both S_s and S_l tend to saturate at an almost constant value for $F \gg F_t$. In Fig. 2(c) we find that there is smectic QLRO [5,6,12] with a value of $0.5 < \sigma_G < 0.7$. However, we were not able to obtain a reliable finite size analysis for the longitudinal peaks since they have large fluctuations from size to size. Also, we find hysteresis in S_s around F_t when decreasing F.

A better understanding of the *dynamical* transitions can be obtained from studying the temporal behavior of the system in both directions. It has been observed experimentally that the longitudinal voltage can show low frequency noise [20,21]. This voltage noise reaches a very large value above the critical current, which has been attributed to plastic flow [21], and then the noise decreases for large current. In addition, even when the total dc transverse voltage $\langle V_x \rangle = \langle \frac{1}{N_v} \sum_i \frac{dx_i}{dt} \rangle$ is zero, it can also have fluctuations and noise [23]. In fact, it is easy to understand that this *Hall noise* will be closely related to the wandering and wiggling of the plastic flow channels and to the jumps between elastic channels in the smectic phase. We have calculated the power spectrum of both the longitudinal voltage, $S_y(f) = \frac{1}{T} |\int_0^T dt\, [V_y(t) - V] \exp(i2\pi ft)|^2$, and the transverse voltage, $S_x(f) = \frac{1}{T} |\int_0^T dt\, V_x(t) \exp(i2\pi ft)|^2$. The low frequency noise is defined as $P_{x,y} = \lim_{f \to 0} S_{x,y}(f)$. In Fig. 3(a) we show the values of the longitudinal noise P_y and the Hall noise P_x as a function of the force ($P_{x,y}$ were approximated from the average of the ten lowest frequencies). We see that, near the critical force, the longitudinal noise is large while the Hall noise is 1 order of magnitude smaller. In this regime of plastic flow the noise is dominated by fluctuations in the direction of motion and by channel tortuosity [4], and since there are few channels the Hall noise is small. When the number of channels increases the vortices wander more in the x direction and the Hall noise increases. At F_p the voltage noise becomes isotropic, $P_x = P_y$. This is the point where we have seen the highest interconnection in the channel network. The coincidence of isotropic noise, onset of short-range smectic order, and peak in differential resistance suggest that there is a dynamic transition at F_p, although a crossover between two flow regimes cannot be discarded. Above F_p, the onset of elastic channels and smectic ordering reduces the longitudinal noise, while the Hall noise remains large due to the "activated" jumps between elastic channels. At F_t the Hall noise falls abruptly, nearly 2 orders of magnitude. This corresponds to a *freezing transition* of vortex motion in the transverse direction. Above F_t there are no more vortex jumps between elastic channels. The low frequency noise can be closely related to diffusive motion for large times. We analyze the average quadratic displacements of vortices in both directions from their center-of-mass position $(X_{\rm cm}(t), Y_{\rm cm}(t))$ as a function of time. We define $w_x(t) = \frac{1}{N_v} \sum_i [\tilde{x}_i(t) - \tilde{x}_i(0)]^2$ and $w_y(t) = \frac{1}{N_v} \sum_i [\tilde{y}_i(t) - \tilde{y}_i(0)]^2$, where $\tilde{x}_i(t) = x_i(t) - X_{\rm cm}(t)$, $\tilde{y}_i(t) = y_i(t) - Y_{\rm cm}(t)$. We observe that

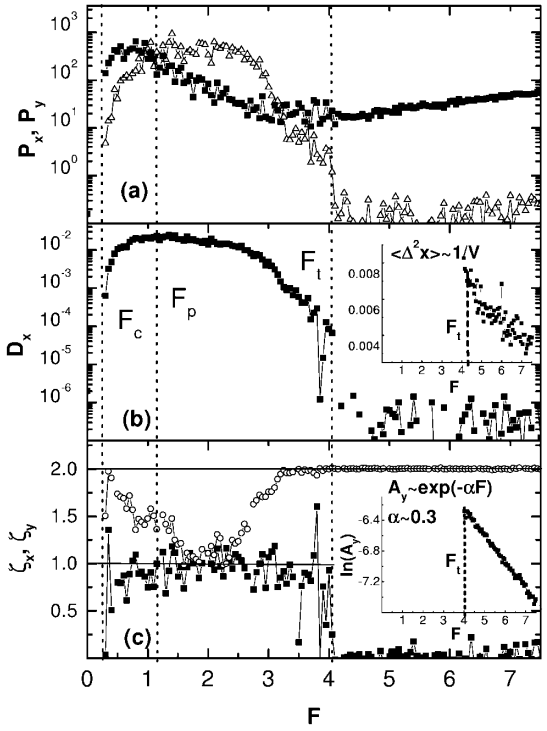

FIG. 3. (a) Low frequency voltage noise vs F. Longitudinal voltage noise P_y, black points. Hall noise P_x, white points. (b) Diffusion coefficient for transversal motion D_x. The inset shows the average transverse quadratic displacement $\langle \Delta^2 x \rangle$ in the frozen phase, $F > F_t$. (c) Diffusion exponents ζ_x (black dots) and ζ_y (white dots) defined from $\langle [\tilde{x}(t) - \tilde{x}(0)]^2 \rangle \sim t^{\zeta_x}$, $\langle [\tilde{y}(t) - \tilde{y}(0)]^2 \rangle \sim t^{\zeta_y}$. The inset shows a plot of A_y defined from a fit $\langle [\tilde{y}(t) - \tilde{y}(0)]^2 \rangle = A_y t^2$ for $F > F_t$.

the vortex motion for $F_c < F < F_t$ is diffusive in the transverse direction, $w_x(t) \sim D_x t$. In Fig. 3(b) we show the behavior of the transverse diffusion coefficient D_x. It closely follows the behavior of the Hall noise, $D_x \propto P_x$. The transverse diffusion is maximum at the peak in the differential resistance F_p and it has an abrupt jump to zero at F_t, indicating the transverse freezing transition. It is interesting to note that melting transitions also show a jump in the diffusion coefficient. Above F_t, the transverse wandering is independent of time since vortex motion is localized in the x direction: $w_x(t) \approx \langle \Delta^2 x \rangle$. In the inset of Fig. 3(b) we show $\langle \Delta^2 x \rangle$ vs F for $F > F_t$. We find that $\langle \Delta^2 x \rangle \approx 0.02a^2$ at F_t, consistent with a Lindemann criterion for melting [7]. Since the diffusion coefficient of free Brownian particles is $D \propto T$ (and it is a monotonous function of T in a liquid) we can interpret D_x as a rough measure of an "effective temperature" T_{eff} below F_t. Similarly, above F_t we can think that $\langle \Delta^2 x \rangle \sim T_{\text{eff}}$. Indeed, we obtain $\langle \Delta^2 x \rangle \sim 1/F$, which is consistent with $T_{\text{eff}} \propto 1/V$ [1,7].

The long-time behavior is better understood by studying the diffusion exponents $w_x(t) \sim t^{\zeta_x}$ and $w_y(t) \sim t^{\zeta_y}$. In Fig. 3(c) we show the behavior of $\zeta_{x,y}$. We see that, for $F_c < F < F_t$, $\zeta_x \approx 1$ corresponding to normal diffusion, while for $F > F_t$, $\zeta_x \approx 0$ corresponding to the freezing of transverse motion. More interestingly, the motion in the longitudinal direction is always superdiffusive, $\zeta_y > 1$. Above F_t, in the frozen phase, the longitudinal fluctuations become *ballistic*, $\zeta_y \approx 2$. Since the vortex positions are localized in the x direction, we see that $w_y(t) = \langle [y(t) - y(0)]^2 \rangle \approx A_y t^2$, with $A_y = \langle \Delta^2 v_y \rangle$ the dispersion of the average velocities of the elastic channels. In the inset of Fig. 3(c) we find that A_y decreases exponentially with the force $A_y \sim \exp(-\alpha F)$. [This suggests a "thermal" distribution of channel velocities; since $T_{\text{eff}} \sim 1/F$, then $\langle \Delta^2 v_y \rangle \sim \exp(-\alpha'/T_{\text{eff}})$.] In the smectic flow region an exponent $1 < \zeta_y < 2$ can be explained by assuming that vortices move most of the time in the elastic channels and occasionally have diffusive jumps between channels in the transverse direction.

In conclusion, we have obtained evidence of two dynamical phase transitions which can be verified experimentally by measurements of voltage noise *and Hall noise*. The first transition at F_p is the point of isotropic noise and maximum transverse diffusion (i.e., maximum effective temperature) and corresponds to the observed peak in the differential resistance. The second transition at F_t is a freezing transition in the *transverse* direction, where the transverse diffusion vanishes abruptly and the Hall noise drops many orders of magnitude.

We acknowledge discussions with A. R. Bishop, P. Cornaglia, Y. Fasano, F. de la Cruz, S. Bhattacharya, V. B. Geshkenbein, F. Pardo, V. M. Vinokur, M. B. Weissman, and G. Zimányi. This work has been supported by a grant from ANPCYT (Argentina) and partially by Fundación Antorchas, Conicet, and CNEA. Parts of this work were performed under the auspices of the U.S. D.O.E.

[1] A. E. Koshelev and V. M. Vinokur, Phys. Rev. Lett. **73**, 3580 (1994).
[2] H. J. Jensen *et al.*, Phys. Rev. Lett. **60**, 1676 (1988); A.-C. Shi and A. J. Berlinsky, Phys. Rev. Lett. **67**, 1926 (1991); A. E. Koshelev, Physica (Amsterdam) **198C**, 371 (1992); M. C. Faleski *et al.*, Phys. Rev. B **54**, 12 427 (1996); C. Reichhardt *et al.*, Phys. Rev. Lett. **78**, 2648 (1997).
[3] N. Grønbech-Jensen, A. R. Bishop, and D. Domínguez, Phys. Rev. Lett. **76**, 2985 (1996).
[4] C. J. Olson, C. Reichhardt, and F. Nori, Phys. Rev. Lett. **80**, 2197 (1998).
[5] T. Giamarchi and P. Le Doussal, Phys. Rev. Lett. **76**, 3408 (1996); P. Le Doussal and T. Giamarchi, Phys. Rev. B **57**, 11 356 (1998).
[6] L. Balents, M. C. Marchetti, and L. Radzihovsky, Phys. Rev. B **57**, 7705 (1998).
[7] S. Scheidl and V. M. Vinokur, Phys. Rev. E **57**, 2574 (1998); Phys. Rev. B **57**, 13 800 (1998); Phys. Rev. B **56**, R8522 (1997); I S. Aranson, S. Scheidl, and V. M. Vinokur, Phys. Rev. B **58**, 14 541 (1998).
[8] S. Bhattacharya and M. J. Higgins, Phys. Rev. Lett. **70**, 2617 (1993); Phys. Rev. B **52**, 64 (1995); M. J. Higgins and S. Bhattacharya, Physica (Amsterdam) **257C**, 232 (1996).
[9] M. C. Hellerqvist *et al.*, Phys. Rev. Lett. **76**, 4022 (1996).
[10] U. Yaron *et al.*, Nature (London) **376**, 743 (1995).
[11] F. Pardo *et al.*, Nature (London) **396**, 348 (1998).
[12] K. Moon, R. T. Scalettar, and G. Zimányi, Phys. Rev. Lett. **77**, 2778 (1996).
[13] S. Ryu *et al.*, Phys. Rev. Lett. **77**, 5114 (1996).
[14] S. Spencer and H. J. Jensen, Phys. Rev. B **55**, 8473 (1997).
[15] C. J. Olson, C. Reichhardt, and F. Nori, Phys. Rev. Lett. **81**, 3757 (1998).
[16] D. Domínguez, Phys. Rev. Lett. **82**, 181 (1999).
[17] D. Domínguez, N. Grønbech-Jensen, and A. R. Bishop, Phys. Rev. Lett. **78**, 2644 (1997).
[18] I. Aranson, A. Koshelev, and V. Vinokur, Phys. Rev. B **56**, 5136 (1997).
[19] L. Balents and M. P. A. Fisher, Phys. Rev. Lett. **75**, 4270 (1995).
[20] W. J. Yeh and Y. H. Kao, Phys. Rev. B **44**, 360 (1991).
[21] A. C. Marley *et al.*, Phys. Rev. Lett. **74**, 3029 (1995); R. D. Merithew *et al.*, Phys. Rev. Lett. **77**, 3197 (1996); M. W. Rabin *et al.*, Phys. Rev. B **57**, R720 (1998); T. Tsuboi *et al.*, Phys. Rev. Lett. **80**, 4550 (1998).
[22] N. Grønbech-Jensen, Int. J. Mod. Phys. C **7**, 873 (1996); Comput. Phys. Commun. (to be published).
[23] N. Grønbech-Jensen *et al.*, Phys. Rev. B **46**, 11 149 (1992).